

# **GaAs/AlGaAs MULTI-QUANTUM-WELL BASED FAR INFRARED DETECTORS FOR ASTRONOMY APPLICATION**

S. V. Bandara, S. D. Gunapala, D. Z-Y. Ting, S. B. Rafol, and J. K. Liu  
Jet Propulsion Laboratory  
California Institute of Technology  
Pasadena, California

## **ABSTRACT**

We are developing a novel GaAs/AlGaAs multi-quantum-well (MQW) far infrared detector based on intersubband absorption in shallow quantum wells. This type of MQW detectors and large format focal plane arrays (FPAs) have been successfully demonstrated in the mid and long-wavelength infrared (LWIR) region up to 27 microns. The carrier relaxation process of these far infrared detectors are limited by the longer life-time associated with longitudinal-acoustic phonon emission process, compared to the faster relaxation process in mid- and LWIR MQW detectors. As a result, the far infrared detectors should exhibit a higher responsivity than mid- and LWIR MQW detectors. Preliminary theoretical estimates show that MQW based, far infrared detectors with a 70 microns cutoff wavelength can operate at around 7 K with detectivity ( $D^*$ ) exceeding  $1 \times 10^{11}$  Jones. As a result of mature GaAs growth and processing technology, thermal IR detectors based on this technology have already demonstrated very high uniformity ( $< 0.02\%$ ), operability ( $> 99.99\%$ ), very low  $1/f$  noise knee ( $< 10$  mHz) in large format ( $1024 \times 1024$ ) focal planes. Thus, we strongly believe large format FPAs of these far infrared detectors can be achievable in the near future.

## **INTRODUCTION**

Quantum Well Infrared Photodetectors (QWIPs) operate by the photoexcitation of electrons between the ground and first excited states' subbands of multi-quantum wells (MQWs) which are artificially fabricated by placing thin layers of two different, high-bandgap semiconductor materials alternately<sup>1,2</sup>. The bandgap discontinuity of two materials creates quantized subbands in the potential wells associated with conduction bands or valence bands. The structure parameters are designed so that the photo-excited carriers can escape from the potential wells and be collected as photocurrent (See Figure 1). QWIPs possess greater flexibility than the usual, extrinsically-doped semiconductor IR detectors. The wavelength of the peak response and cutoff can be continuously tailored, over a wide wavelength range, by varying the quantum well thickness and the barrier height. The lower detection wavelength is limited by the spreading of the bandgap discontinuity of the two materials system used in the detector. However, theoretically there is no limit in the upper detection wavelength, because one can design a very shallow quantum well using a slightly different material combination<sup>1</sup>. Accurate fabrication of such a device requires precious control in material flux during the growth.

The lattice matched GaAs/ $\text{Al}_x\text{Ga}_{1-x}\text{As}$  material system is commonly used to create a QWIP structure similar to the one shown in Figure 1(a). Highly uniform, pure crystal layers of such semiconductors can be grown on large substrate wafers up to 6" diameter, with control of each layer thickness down to a fraction of a molecular layer, using such modern crystal-growth methods as molecular beam epitaxy (MBE). Thus, by controlling the quantum well width (GaAs layer thickness) and the barrier height (which depends on the Al molar ratio of  $\text{Al}_x\text{Ga}_{1-x}\text{As}$  alloy), this intersubband transition energy can be varied over a wide enough range to enable light detection at any wavelength range from  $\lambda > 4 \mu\text{m}$ . Infrared detectors sensitive up to a 27  $\mu\text{m}$  wavelength have been demonstrated using GaAs/ $\text{Al}_x\text{Ga}_{1-x}\text{As}$  based QWIPs<sup>1-6</sup>. One of the early criticisms of QWIP technology is the narrow bandwidth of the responsivity spectrum. By replacing single quantum wells with small superlattice structures (several quantum wells separated by thin barriers) in the multi-quantum well structure, JPL has recently developed a technique to design a broadband QWIP<sup>3</sup>. Such a scheme creates an excited state miniband, due to overlap of the excited state wave functions of quantum wells. Figure 1(b) shows experimentally measured narrow and broadband responsivity spectra in 6-20  $\mu\text{m}$  range.

Contact information for S.V. Bandara: Email: [Sumith.V.Bandara@jpl.nasa.gov](mailto:Sumith.V.Bandara@jpl.nasa.gov)

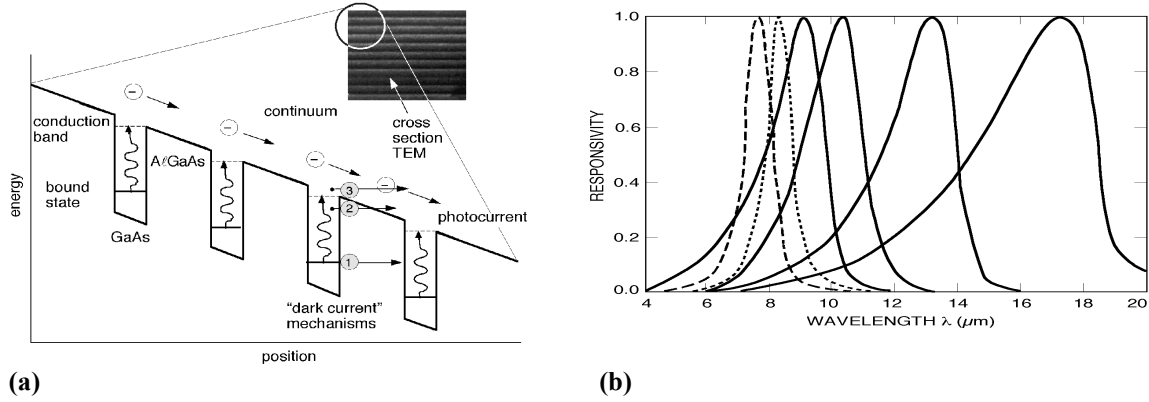


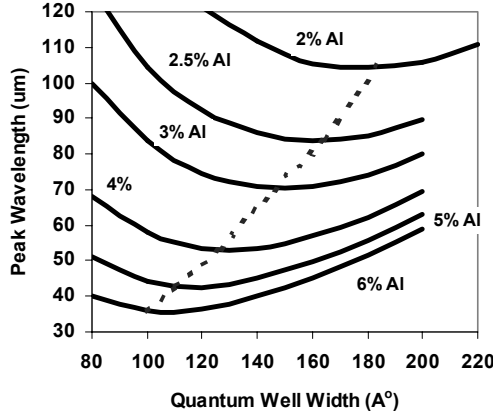
Figure 1 (a). Schematic diagram of the conduction band in a bound-to-quasibound QWIP in an externally applied electric field. Absorption of IR photons can photoexcite electrons from the ground state of the quantum well into the continuum, causing a photocurrent. Three dark current mechanisms are also shown: ground state tunneling, thermally assisted tunneling, and thermionic emission . (b). Spectral coverage and tailorability of QWIPs in 4-20  $\mu\text{m}$  wavelength range.

### GaAs/AlGaAs FIR QWIPs

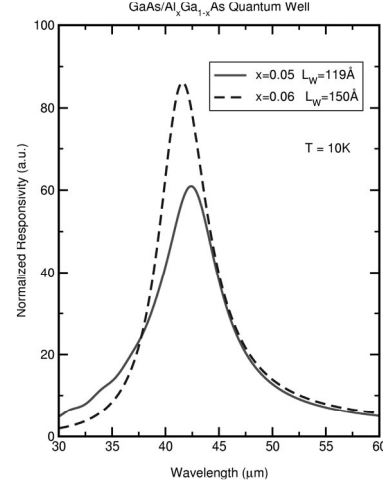
Absorption peak wavelength ( $\lambda_p$ ) of intersubband transitions in quantum wells is simply determined by the ground ( $E_0$ ) and excited ( $E_1$ ) state energy difference. Typical calculations of  $E_0$  and  $E_1$  require only basic quantum mechanics and boundary conditions linking envelope wave functions of the well and barrier sides of the heterointerface<sup>1,2</sup>. For a quantum well with finite barrier, one can write exact wave functions for the ground and excited state wave functions in both well and barrier regions, and evaluate the absorption peak and oscillator strength. Figure 2(a) shows the numerical calculations of  $\lambda_p$  as a function of quantum well width for shallow GaAs/ $\text{Al}_x\text{Ga}_{1-x}\text{As}$  quantum wells. As shown in the Figure 2, one can easily design a detector with a peak absorption wavelength of up to 100  $\mu\text{m}$  using low Al compositions ( $x$ ) in the barriers. Although these quantum wells have large optical dipole moments, this, by itself, is not useful for detection unless photoexcited carriers readily escape from the excited state. For bound-to-bound transitions, where both ground and excited states are classically bound within the well, escaping of the photoexcited electrons will be partly suppressed due to the barrier height seen by the electrons in the excited state. By decreasing the width or barrier height of a quantum well that contains two bound states, the excited bound state can be pushed into the continuum, resulting in a larger escape probability of photoexcited electrons. However, this situation can increase the unwanted dark current of the detector. Therefore, the optimum design is to place the excited state exactly at the well top, which is referred as bound-to-quasibound design, where the signal to noise ratio is maximized<sup>1,4,5</sup>. A dashed line in Figure 2(a) corresponds the bound-to-quasibound QWIP for given well width and Al composition.

### WAFER FABRICATION AND CHARACTERIZATION

Practically controlling and repeating low Al composition during the MQW growth is difficult, and requires the recalibration of Al/Ga sources in the MBE chamber. Using an existing MBE system, we have fabricated two QWIP wafers with shallow quantum wells, on semi-insulating GaAs substrates. These wafers consists of 30 period GaAs multiquantum wells bounded by  $x = 0.05$  (5%) and  $x = 0.06$  (6%)  $\text{Al}_x\text{Ga}_{1-x}\text{As}$  barriers. The well width of each detector is 120  $\text{\AA}$  and 150  $\text{\AA}$ , respectively. The central sections of the quantum wells (30 $\text{\AA}$  away from the barriers) are doped with Si impurities up to a density of  $2 \times 10^{17} \text{ cm}^{-3}$ . The samples consist of these device structures, sandwiched between two contact layers. Figure 2(b) shows the calculated absorption spectra of the devices. As expected, bound-to-bound QWIP shows narrower spectra than bound-to-quasibound QWIP.



(a)



(b)

Figure 2. (a). Numerical calculations of  $\lambda_p$  as a function of quantum well width for shallow GaAs/Al<sub>x</sub>Ga<sub>1-x</sub>As quantum wells with different Al compositions. The dashed line shows bound-to-quasi design where excited state resonance with the barrier top. (b). Shows the simulated absorption spectra for two different QWIPs with parameters shown in the Table 1.

In order to test the existence of the barriers, 200 μm diameter mesas were fabricated using wet chemical etching, and evaporating Au/Ge ohmic contacts onto the top and bottom contact layers. Figure 3 shows the estimated work function for thermionic emission for different bias voltages. These were calculated using Arrhenius plots, obtained by measuring thermal dark currents at different bias voltages and different temperatures. At zero bias voltage, work function is given by:  $\Delta E = E_B - E_0 - E_F$ , where  $E_B$  is the barrier height,  $E_0$  is the ground state energy and  $E_F$  is the fermi level in the quantum well. Table 1 shows an excellent agreement between the estimated and measured values of the work function, confirming the existence of the Al<sub>x</sub>Ga<sub>1-x</sub>As barriers.

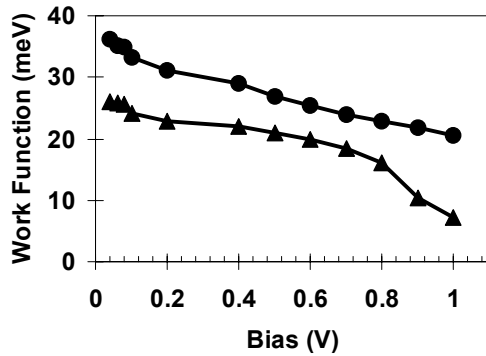


Figure 3: The workfunction vs bias voltage for two QWIP wafers described in Table 1. As expected both quantum well barriers show effective barrier lowering due to applied bias voltage.

## DISCUSSION AND CONCLUSION

Optical responsivity of far IR QWIPs are expected to perform better than the thermal IR QWIPs, due to the different carrier relaxation mechanisms associated with each case. Energy relaxation in a quantum well with more than one bound state is mainly controlled by the intersubband lifetime  $\tau_s$ . For transition energies greater than optical phonon energy, the intersubband lifetime, which is limited by the optical phonon

emission, is very short ( $\tau_s < 1$  ps). For transitions energies below optical phonon energy, this time is now limited by the emission of acoustic phonons, which is much longer<sup>7,8</sup>. For GaAs material system, optical phonon energy is  $\sim 36$  meV, which corresponds to wavelength  $\lambda \sim 34$   $\mu\text{m}$ . Therefore, for far IR ( $\lambda > 34$   $\mu\text{m}$ ) QWIPs, this situation opens the possibility of a “phonon bottleneck effect” for photoexcited electrons, which may remain in an excited state with a longer lifetime, resulting in a higher optical gain and responsivity. Preliminary theoretical estimates show that these MQW based, far infrared detectors, with 70 microns cutoff wavelength, can operate at  $\sim 7$  K with a detectivity ( $D^*$ ) exceeding  $1 \times 10^{11}$  Jones.

**TABLE 1:** Design parameters of two QWIPs for FIR detection and comparison of calculated and experimentally obtained barrier workfunctions ( $\Delta E$ ).

Al%	Well Width	Well doping Density	$E_B$ MeV	$E_0$ meV	$E_F$ meV	Theory $\Delta E$ meV	Experiment $\Delta E$ meV
5%	120 Å	$1.2 \times 10^{11} \text{ cm}^{-2}$	44.5	14.3	4.3	25.9	$\sim 27$
6%	150 Å	$1.8 \times 10^{11} \text{ cm}^{-2}$	53.3	11.5	6.4	35.4	$\sim 37$

The foremost advantage of QWIP technology is that it can provide highly uniform and steady Focal Plane Arrays (FPAs) in larger formats with pixel operability exceeding 99.9%, due to highly matured fabrication and processing technologies<sup>4,5,9-11</sup>. These FPAs show excellent  $1/f$  noise properties ( $1/f$  noise knee  $< 30$  mHz), allowing longer integration times without calibration. Recently, we obtained excellent astronomical images when operating an infrared camera with a  $256 \times 256$  QWIP array sensitive at  $8.5$   $\mu\text{m}$  at the prime focus of the 5-m Hale telescope. The remarkable noise stability – and low  $1/f$  noise – of QWIP focal plane arrays enable camera to operate by modulating the optical signal with a mod period up to 100 s. A 500 s observation on dark sky renders a flat image, with little indication of the low spatial frequency structures associated with imperfect sky subtraction or detector drifts<sup>11,12</sup>. Such unique properties of the FPA remarkably simplifies the on-board data analysis, thus providing significant cost reduction in software development, data processing and major system level benefits upon integration. In addition, recent demonstration of the simultaneously readable, dual band,  $640 \times 486$  QWIP FPA will provide innovative ways to simplify IR sensing instruments<sup>10</sup>.

## REFERENCES

1. S. D. Gunapala, S. V. Bandara, *Physics of Thin Films*, edited by M. H. Francombe, and J. L. Vossen, Vol. **21**, 113, Academic Press, NY, 1995.
2. B.F. Levine, *J. Appl. Phys.* **74**, R1 (1994).
3. S. V. Bandara, S. D. Gunapala, J. K. Liu, E. M. Luong, J. M. Mumolo, W. Hong, D. K. Sengupta, and M. J. McKelvey, *Appl. Phys. Lett.* **72**, 2427 (1998).
4. S. D. Gunapala and S. V. Bandara, *Semiconductors and Semimetals*, **62**, 197-282, Academic Press, 1999.
5. S. D. Gunapala, S. V. Bandara, J. K. Liu, W. Hong, M. Sundaram, P. D. Maker, R. E. Muller, R. Carralejo, and C. A. Shott, *IEEE Trans. Elec. Devices*, **45**, 1890 (1998).
6. A. G. U. Perera, W. Z. Shen, S. G. Matsik, H. C. Liu, and M. Buchanan, and W. J. Schaff, *Appl. Phys. Lett.* **72**, 1596 (1998).
7. J. Faist, C. Sirtori, F. Capasso, L. Pfeiffer, and K. W. West, *Appl. Phys. Lett.* **64**, 872 (1994).
8. J. Faist, F. Capasso, C. Sirtori, D. L. Sivco, A. L. Hutchinson, S. N. G. Chu, and A. Y. Cho, *Appl. Phys. Lett.* **63**, 1354 (1993).
9. S. V. Bandara, S. D. Gunapala, J. K. Liu, S. B. Rafol, D. Z. Ting, J. M. Mumolo, F. M. Reininger, J. M. Fastenau, and A. K. Liu, *SPIE Proceedings*, **4454**, 30 (2001).
10. S. D. Gunapala, S. V. Bandara, A. Singh, J. K. Liu, S. B. Rafol, E. M. Luong, J. M. Mumolo, N. Q. Tran, J. D. Vincent, C. A. Shott, J. Long and P. D. LeVan, *IEEE Trans. Elec. Devices*, **47**, 963 (2000).
11. S. V. Bandara, S. D. Gunapala, J. J. Bock, M. E. Ressler, J. K. Liu, E. M. Luong, J. M. Mumolo, S. B. Rafol, D. Z. Ting, and M. W. Werner, *SPIE Proceedings*, **4008**, 1298 (2000).
12. M. E. Ressler, J. J. Bock, S. V. Bandara, S. D. Gunapala, and M. W. Werner, *Infrared Physics & Tech.*, **42**, 377 (2001).